

# RE-EVALUATION OF THE STRAIN CONCENTRATION FACTOR THROUGH ELASTO-PLASTIC ANALYSES

DAN MIHAI CONSTANTINESCU<sup>1</sup>, MARIN SANDU<sup>1</sup>, LIVIU MARSAVINA<sup>2</sup>,  
MATEI CONSTANTIN MIRON<sup>1</sup>, RADU NEGRU<sup>2</sup>, DRAGOS ALEXANDRU APOSTOL<sup>1</sup>

*Abstract.* Digital image correlation and three-dimensional finite element investigations are done for analyzing strain concentration for a semicircular notch and two V-notches with different radii. Along the notch bisector normalized true opening strains are represented as a function of the normalized distance from the notch root. In the linear elastic domain a comparison to an analytical solution is also done. Strain variations in the elasto-plastic domain show that the experimental normalized strains are greater than the numerical ones, both close to the notch root and over the whole ligament. The calculation of an effective strain concentration factor for V-notches is done and its variation based on experimental results proves to be much closer to real phenomena of strain distribution in the elasto-plastic domain.

*Key words:* digital image correlation, elasto-plastic strain variation, finite elements, effective strain concentration factor, V-notches.

## 1. INTRODUCTION

For the linear analysis of plane cases, the use of complex potential functions together with bi-harmonic potential functions established main contributions for sharp notches due to the solutions of Westergaard [1] and Irwin [2]. The sharp V-shaped notch solution due to Williams [3] has been completed by the solution for blunt cracks proposed by Creager and Paris [4], and then by Glinka [5] who established closed-form expressions to the generalized stress intensity factors (SIFs) in the Creager-Paris' equations. Around the notch tip, where stress distributions depend essentially on the notch tip radius, such equations continue to be a very powerful tool of analyzing the stress fields intensity. For sharp and rounded V-notches, Lazzarin and Tovo [6] gave a solution capable of addressing any combination of notch tip radius and opening angle. This approximate solution showed lack of accuracy in describing the stress field for the rounded V-shaped notches with a large opening angle. Afterwards, Lazzarin et al. [7] extended that approach in order to take also into account the influence of plate finite size on the stress fields ahead the stress raiser. Other formulations already reported in the literature by Glinka and Newport [8], Xu *et al.* [9], and Kujawski and Shin [10],

---

<sup>1</sup> "Politehnica" University of Bucharest, Splaiul Independenței nr. 313, 060042 Bucharest

<sup>2</sup> "Politehnica" University of Timișoara, B-dul Mihai Viteazul nr. 1, 300222 Timișoara

have also focused on the maximum principal stress distribution along the notch bisector, which is of great interest in engineering applications.

Filippi *et al.* [11] developed new equations adding to the previous solution [6] a potential function capable to improve the term that has influence on the stress distribution close to the notch tip. Berto *et al.* [12] compared the equations proposed by Filippi *et al.* [11] to the Neuber's solution [13, 14] valid for sharp notches with an arbitrary opening angle. As the original formulation due to Neuber by using a conformal mapping representation described only the normal stress along the notch bisector it was shown that the Filippi's solution is more complete and is capable also to describe the stress components outside the notch bisector. In [12] it is demonstrated that Filippi's stress equations for tension-loaded V-notches are giving better results than Neuber's equations, the latter even in an amended form. This is confirmed by comparison with highly accurate FE results obtained for different notch radii and notch opening angles. It is also shown that in the case of out-of-plane shear loading, Neuber's original solution is highly accurate and needs no amendment.

The problem of establishing the three-dimensional stress fields near a cut-out or notch in a plate of finite thickness is very complex because of the difficulty in precisely satisfying the boundary conditions. Plane stress and plane strain conditions are applicable only when the plates are either very thin or very thick, respectively. In particular, due to the presence of the notch tip radius, it is not clear whether the notch-tip stress field is close to that of plane stress or plane strain, especially when the notch tip radius is small as compared to plate thickness (Li *et al.* [15], Li and Guo [16]). As mentioned by Kotousov and Wang [17], no solutions are currently available for the through-the-thickness stress components, which strongly affect the notch-tip plastic deformation, and may play a very important role in any strain energy density-based calculation as to establish the size of the plastic zone ahead the notch tip. As it is well known, there exists at the vicinity of a V-shaped notch root a three-dimensional deformation field influenced by four parameters which are: the notch tip radius, the notch depth, the notch angle and the plate thickness. The influence of these parameters was examined in [16] using detailed 3D finite element analyses.

When establishing singular stress and deformation fields ahead of cracks and pointed V-notches in materials with a nonlinear elastic behaviour one should pay a special tribute to the papers of Hutchinson [18] and Rice and Rosengren [19] who expressed for mode I and II in the 'HRR solution' the crack tip fields for stresses and strains as a function of the dominant term or the  $J$ -integral. In a paper by Lazzarin *et al.* [20] the Plastic Notch Stress Intensity Factors (NSIFs) are used to express the terms of the stress field parameters and thought as an extension of the linear elastic NSIFs previously defined by Gross and Mendelson [21]. Within this context, by reformulating the Equivalent Strain Energy Density (ESED) criterion proposed by Molski and Glinka [22] for pointed V-notches in plates subjected to tension or bending loading and plane strain conditions, Lazzarin and Zambardi [23]

gave the plastic NSIFs as a function of the linear elastic ones. In order to obtain this link, they formulated the hypothesis that under plane strain conditions the concentration of the strain energy density, as evaluated over a structural volume surrounding the pointed V-notch tip, was constant. Such a volume has to be fully contained in the zone where stress fields can be satisfactorily predicted by a one-term asymptotic law. It was also underlined that when small scale yielding conditions are present, this hypothesis immediately results in the constancy of the mean value of the strain energy density.

Sethuraman and Viswanadha [24] developed a simplified analytical method based on Neuber's rule for the calculation of the actual elasto-plastic stress-strain state at the tip of a notch, subjected to general loading. The methodology is very similar to that proposed by Singh *et al.* [25], but in their study it is proposed that the actual total strain energy density, corresponding to the elasto-plastic state at the stress concentration point is proportional to the total hypothetical elastic strain energy density. This proportionality factor is introduced in their model, [24], in order to account for stress relaxation and redistribution. Initially, the method is used for Mises materials obeying a bi-linear hardening rule and later the application has been extended for a general hardening material by treating the material as with multilinear hardening. The accuracies of the existing analytical methods have been evaluated for various notch geometries, subjected to various loadings and for different material models. The stresses and strains evaluated using the proposed method are in close agreement with the non-linear finite element solutions for all the cases considered. The method based on Neuber's rule predicts an upper bound on the stress and strain values and is found to be safe from the design point of view for the cases considered. For plane strain cases, the ESED method predicts results close to the finite element results and also forms a lower bound for stress and strain values.

Extensive experimental tests have been performed by Gómez *et al.* [26–28] for U- and V-notched PMMA beams loaded under mixed mode. For V-notched beams [28] it is checked the suitability of fracture criteria based on the cohesive zone model and strain energy density when applied to those samples. A very simple fracture criterion based on the dominance of the local mode I for notched samples with different V-notch angles and notch root radii loaded under mixed (I+II) mode is proposed. On the other hand, Kim and Cho [29] presented a unified brittle fracture criterion for cracks and V-notches under mixed mode loading by extending the maximum circumferential stress criterion and Novozhilov's criterion. The mixed mode fracture toughness and crack orientation for tested PMMA plates with a sharp V-notch are predicted by the proposed criterion. Tests were also carried out in order to investigate the mixed mode fracture of the PMMA plates.

The problem of using NSIFs is also analyzed by Susmel and Taylor [30] who presented a number of experimental data obtained from tests conducted on V-notched specimens subjected to in-phase mixed mode I and mode II loadings. Since the mean value of the root radius was very small (0.074 mm) compared to

the other notch dimensions, the notch stress intensity factors were conveniently determined by assuming a notch root radius equal to zero. However, by applying some critical distance methods, the best accuracy was obtained by Susmel and Taylor by taking into account the finite notch root radius, that is, by considering the real-elastic distribution ahead of the tested V-notches. The paper shows that if the process zone governing fracture phenomena is greater than the zone influenced by the tip radius, NSIFs could be directly used to predict failure conditions. The suggestion is to use a generalized form of NSIFs capable of including the influence of the notch root radius and quantifying, in particular, the stress redistribution it involves.

In our work we analyze three symmetric stress raisers in strips loaded in tension: one has a semicircular shape and a radius  $R = 3$  mm, and two are V-notches with radii  $r = 0.5$  mm and  $r = 0.2$  mm. We combine experimental investigations together with finite element analyses. A novel experimental technique is used here for analyzing the elasto-plastic strain fields ahead the notches in a power hardening material. A detailed literature survey of the history of photogrammetry and digital image correlation (DIC) systems is done by Sutton et al. in [31]. In general, DIC is based on the principle of comparing speckle pattern structures on the surface of the deformed and the undeformed specimen or structural component or between any two deformation states. For this purpose, a virtual grid of subsets of a selected size and shape, consisting of certain pixel grey value distributions, is superimposed on the pre-existing or artificially sprayed on surface pattern and followed during deformation by an optical camera system. In this manner, information on the in-plane local strain distribution is gained without assuming a priori the constitutive behaviour of the material. The method finds many applications as in fracture mechanics [32] or fatigue [33] analyses, and its improvements of the sensitivity as discussed in [34] lead to special developments for accurate measurements of the MEMS devices [35]. Detailed three-dimensional (3D) finite element investigations are used to validate the experimental analyses in the nonlinear domain. The tested material is 2024-T3 aluminum which follows a hardening rule of Ramberg-Osgood type. The analyses done on these notches establish mainly the strain variation in the elasto-plastic domain by comparing the true normalized opening strain fields obtained with DIC and 3D finite elements (on the surface and in the midplane) along the notch bisector. Comparison of the obtained normalized strain along the notch bisector in the linear elastic domain with the Filippi's solution gives a good agreement. The variation of a nominal strain concentration factor and of an effective strain concentration factor with the normalized current stress to the offset yielding stress is also presented. In the paper it is also shown that the use of an *effective strain concentration factor* established on experimental bases by dividing at each load level the measured strains at the root of the notches to the strain measured experimentally with a virtual strain gage in the middle of the ligament is to be preferred due to real redistribution strain phenomena in the elasto-plastic domain.

## 2. EXPERIMENTAL TESTING PROCEDURE BY USING DIC

By using the 2M ARAMIS System, the conventional characteristic curve for the material 2024-T3 was obtained for a specimen without notches. Speed of testing was 0.3 mm/min with the force signal acquired directly from a Walter-bai testing machine. Four tests are done and a relevant one is considered for extracting material properties. A longitudinal virtual strain gage was emulated along the axis of symmetry of the specimen and longitudinal conventional strains were obtained without averaging by considering facets of  $25 \times 16$  pixels and a computation size  $7 \times 7$ ; another horizontal virtual strain gage is used for calculating Poisson's ratio. The conventional stress-strain curve is shown in Fig. 1, and the obtained important mechanical properties are: longitudinal modulus of elasticity  $E = 67.85$  GPa, ultimate strength  $\sigma_u = 457$  MPa, offset yield limit  $\sigma_{0.2} = 340$  MPa, elongation at break 17%, and Poisson's ratio 0.35. These are somehow lower than the typical properties provided by the Aluminum Association, Inc. and listed by Matweb, as: longitudinal modulus of elasticity  $E = 71.3$  GPa, ultimate strength  $\sigma_u = 483$  MPa, offset yield limit  $\sigma_{0.2} = 345$  MPa, elongation at break 18%. However, evident deviation from the linear elastic behaviour starts from a stress smaller than 300 MPa, and the limit in between the elastic domain and the plastic domain is at a stress of 260 MPa.

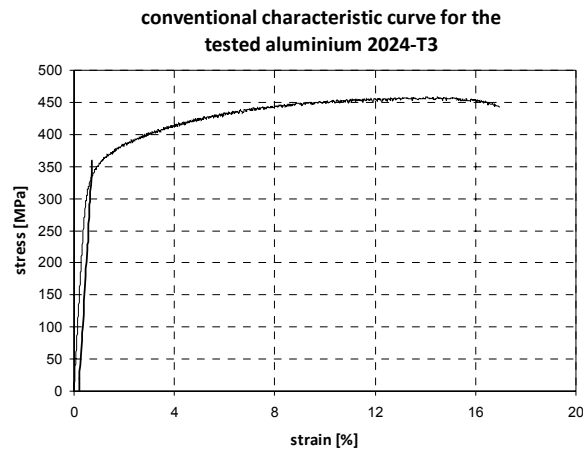


Fig. 1 – Conventional characteristic curve for the tested 2024-T3 aluminum.

Three geometries with symmetrical stress raisers were analyzed (Fig. 2). Specimens have the same length  $L = 120$  mm, width  $H = 20$  mm, and semicircular radius  $R = 3$  mm (Fig. 2a), and two V-notches with an angle of  $90^\circ$  and depth  $a = 3$  mm with radii:  $r = 0.5$  mm (Fig. 2b) and  $r = 0.2$  mm (Fig. 2c). Thickness of the specimens is about 3.2 mm. Longitudinal strains were averaged along the axis of the specimens along virtual strain gages of gage length as 25 mm and 6 mm. These were considered in the middle of each specimen at the location of the three

notches and analyzed during each test. Therefore one can obtain directly values of local longitudinal strains in the net section. For each tested specimen the history of the conventional or true strain variation at the base of each stress raiser was recorded for both of them – left and right as looking towards the specimen – till the failure of the specimens. True strains can be normalized to true elastic strains as to be later compared with finite element results. Calculation of the elastic and elasto-plastic nominal strain concentration factors can be done at each loading step by considering the longitudinal local conventional strains measured at the notch root and along the ligament divided by the nominal conventional strains in the remote cross section area. On the other hand an effective strain concentration factor can be established by considering the same longitudinal local conventional strains measured at the notch root and along the ligament divided by the local conventional strains measured and averaged over a 6 mm virtual strain gage in the middle of the specimen. The size of 6 mm was chosen as being the height of the concentrators at the edge of the specimen for all three geometries.

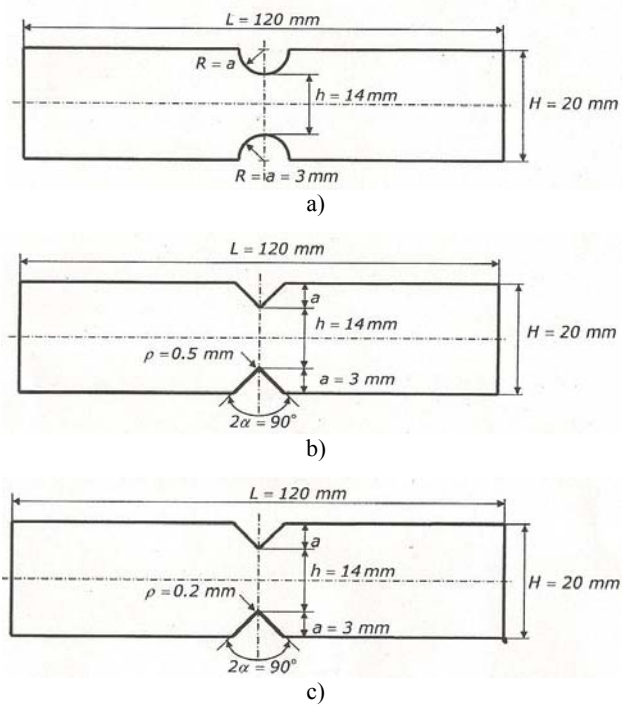


Fig. 2 – Dimensions of specimens with three concentrators: a) semicircular with  $R = 3 \text{ mm}$ ; b) V-notch with  $r = 0.5 \text{ mm}$ ; c) V-notch with  $r = 0.2 \text{ mm}$ .

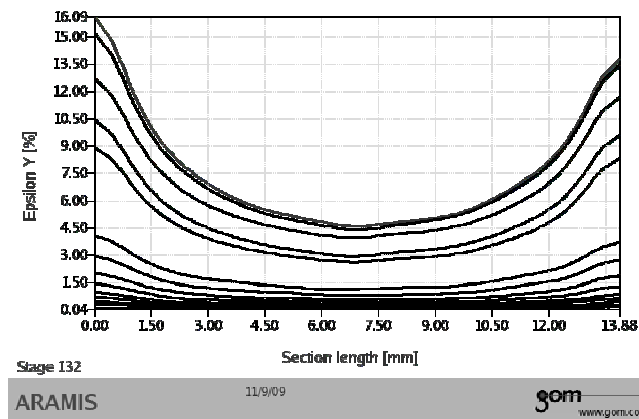
Without getting too much into the details of the use of the digital image correlation method (DIC), we should note that the method is suitable for analyzing local strains at the root of concentrators in elastic and elasto-plastic domains. The

big advantage is that one can obtain the strain values in discrete points as a global field in the ligament area and the variation of the true or conventional normalized strains along a desired line as the notch bisector. Of course that the size of the randomly distributed black dots and the calibration procedure are important for obtaining a good accuracy and avoiding undesired noise during data acquisition. During our tests on the specimens with notches we kept the same settings as: facets of  $20 \times 4$  pixels, computation size  $7 \times 7$ , runs 1 and area  $9 \times 9$ ; only for the specimen with a V-notch having a radius of 0.2 mm filtering was done with runs 3 and an area  $3 \times 3$  was also used. One frame at two seconds was taken.

### 3. EXPERIMENTALLY OBTAINED RESULTS

Strains at the base of the left and right semicircular concentrators and along the notch bisector were measured together with the strains in the middle of the specimen by averaging on two gage lengths of 6 mm and 25 mm. In the linear elastic domain, up to  $\sigma_y = 260$  MPa, it really makes no difference if strains are averaged over 25 mm or 6 mm. At the base of the semicircular notches the strain histories show some noise in the measurements; this is due to the close vicinity to the edge of the specimen when averaging strains over the facets.

When representing the longitudinal (axial)  $\epsilon_y$  strains variation along a section in between the two semicircular notches at different load levels, we can notice (Fig. 3a) that at the left concentrator strains are a little bit higher than at the right concentrator. There is probably some geometry imperfection of the specimen or some misalignment in loading. The measured length of the ligament in between the base of the two notches is in fact 14.022 mm and the difference to 13.88 mm (which is the active measurable length with ARAMIS) represents the “lost” pixels due to the interference of the boundaries. Such small differences will appear also for the other two specimens with different notch geometries.



a)

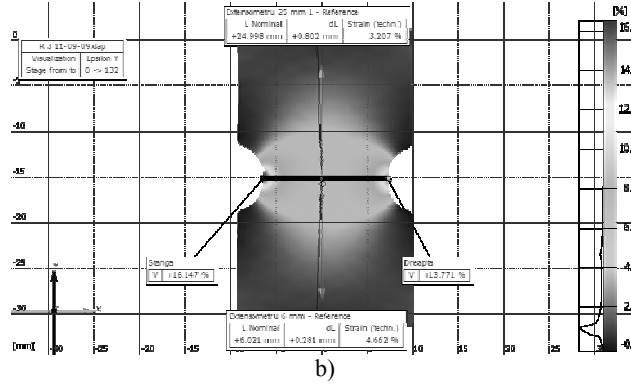


Fig. 3 – Measured  $\epsilon_y$  strains along the section in between semicircular notches: a) for different load levels; b) before failure at 20,692 N.

The forces at which strains are represented are: 3,171 N, 6,197 N, 9,052 N, 11,615 N, 13,835 N, 15,714 N, 16,886 N, 17,813 N, 18,496 N, 20,302 N, 20,180 N, 20,497 N, 20,692 N, and again 20,692 N at the failure of the specimen with a maximum registered strain at the root of the semicircular left notch  $\epsilon_y = 16.15\%$ . In Fig. 3b), the map of the  $\epsilon_y$  strain variation is shown. The value of 16.5% mentioned in the figure is not obtained along the horizontal line but along about a 45° direction, where strain has a maximum.

For the specimen with two V-notches of tip radius  $r = 0.5$  mm some noise is to be measured at the root of the two notches. In Fig. 4 is shown the distribution of the strains measured with DIC in the middle of the specimen with strain gages of 25 mm and 6 mm and at the root of the two notches which is about 6% before failure.

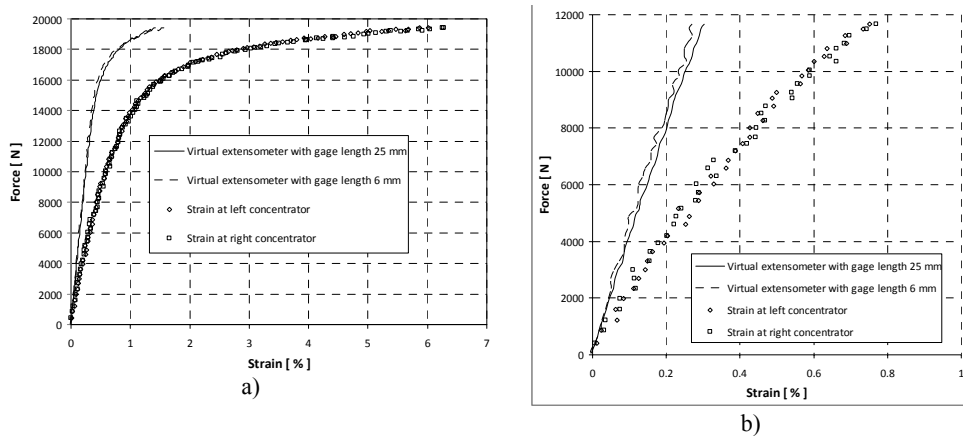


Fig. 4 – History of conventional strains measured by DIC for two V-notches with root radius  $r = 0.5$  mm at notch base and in the middle of the specimen: a) till failure; b) in the linear elastic domain.

Strain distribution in the middle section is more uniform left and right as seen in Fig. 5a). The forces at which strains are represented are: 3,000 N, 6,026 N, 8,760 N, 11,273 N, 13,469 N, 15,373 N, 16,715 N, 17,789 N, 18,447 N, 18,984 N, 19,424 N, and again 19,424 N at the failure of the specimen with a maximum registered strain at the root of the right V-notch  $\varepsilon_y = 6.26\%$ . In Fig. 5b the map of the  $\varepsilon_y$  strain variation is shown. The value of 6.355% mentioned in Fig. 5b is again obtained along a  $45^\circ$  direction where strain has a maximum.

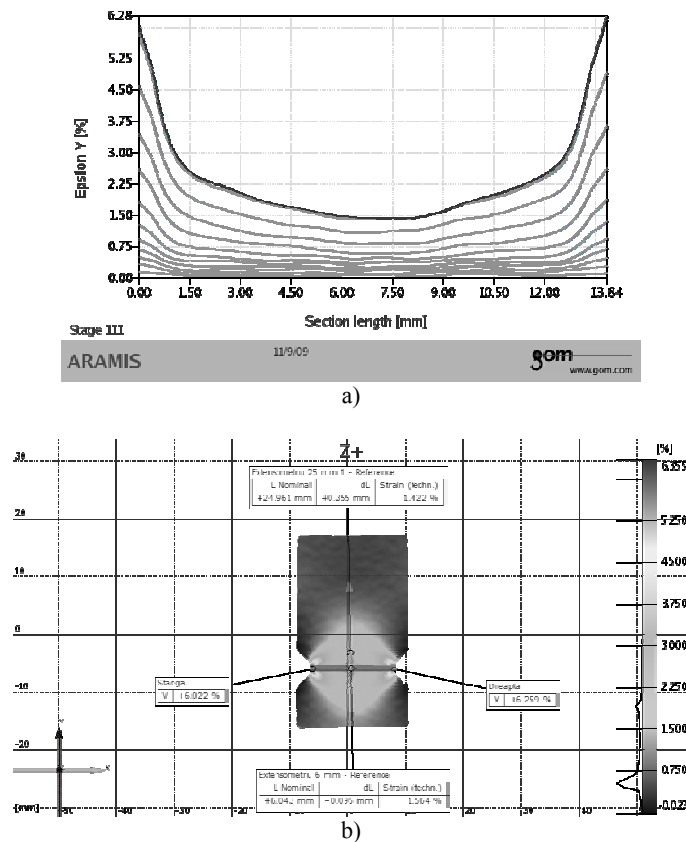


Fig. 5 – Measured  $\varepsilon_y$  strains along the section in between two V notches with  $r = 0.5$  mm: a) for different load levels; b) before failure at 19,424 N.

For the V-notch specimen with notches having a radius  $r = 0.2$  mm, a small area around the contour of the notch roots cannot be analyzed. Strain at the root of the notches is about 4% before failure, smaller than the 6% value obtained for  $r = 0.5$  mm. We have to mention that for this geometry of the notch we used for smoothing the experimentally measured strains filtering with: runs 3 and area  $3 \times 3$ . Strain distribution at the left and right V-notches are to be seen in Fig. 6a. The

forces at which strains are represented are: 3,220 N, 6,270 N, 9345 N, 11,956 N, 14,275 N, 16,129 N, 17,398 N, 18,227 N, and 18,594 N at the failure of the specimen with a maximum registered strain at the root of the right V-notch  $\epsilon_y = 4.03\%$  along a horizontal line section. In Fig. 6b) the map of the  $\epsilon_y$  strain variation is shown. The value of 6.319% mentioned in the figure is obtained on the right notch along a 45° direction where strain has a maximum, and is much bigger than the strain 4.03% measured at the root of the notch. As the root radius becomes smaller the strain becomes more localized along about 45° directions.

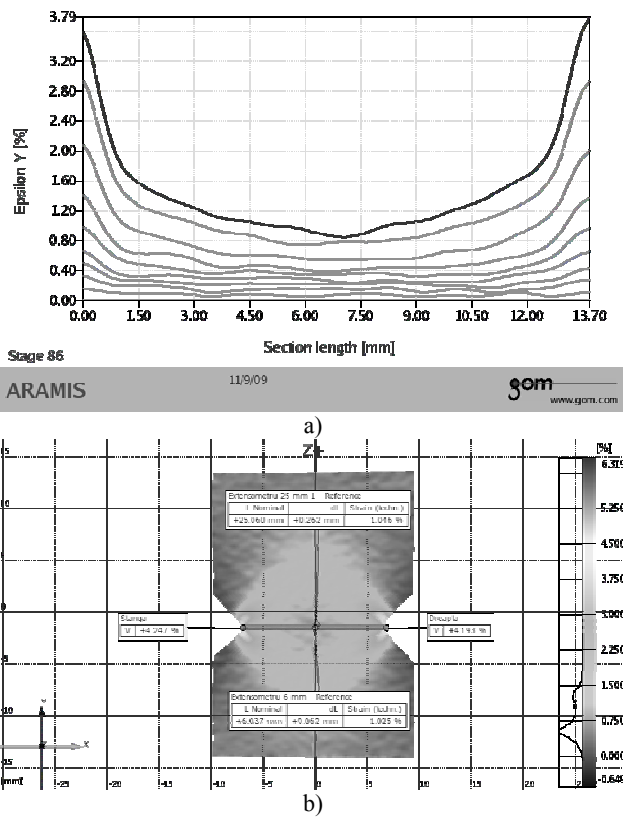


Fig. 6 – Measured  $\epsilon_y$  strains along the section in between two V notches with  $r = 0.2$  mm: a) for different load levels; b) before failure at 18,594 N.

#### 4. COMPARISON OF DIGITAL IMAGE CORRELATION AND FINITE ELEMENT RESULTS

Refined 3D finite element analyses were performed using ABAQUS 6.9.3 software. For all three concentrators about the same size of the mesh was utilized with full integration brick elements. Some details are given for the mesh size of the V-notches starting from the notch root towards the axis of symmetry, along the notch bisector. At the root of the notch there are considered two zones as follows:

for  $r = 0.5$  mm the size of zone 1 is up to 0.5 mm, and in zone 2 from 0.5 mm to 1.5 mm – in zone 1 there are 10 elements of equal width 0.05 mm; in zone 2 there are also 10 elements having a constant width of 0.1 mm; for  $r = 0.2$  mm the size of zone 1 is up to 0.8 mm, and in zone 2 from 0.8 mm to 1.8 mm – in zone 1 there are 10 elements with the first as 0.043 mm and growing progressively to 0.13 mm for the last element; in zone 2 there are also 10 elements having a constant width of 0.1 mm. Afterwards the size of the elements is increased.

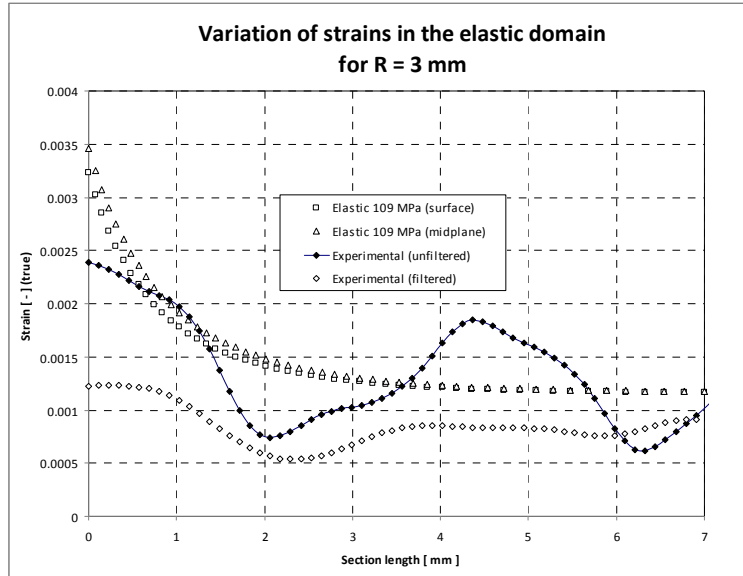
For each tested notched specimen analyses were done both in the elastic and elasto-plastic (using the experimental true stress-true strain curve or Ramberg-Osgood) domains. Results obtained experimentally with DIC and with finite elements are compared in the same plots. We represented the normalized true opening strains in the ligament to the true elastic strains in the gross section (far away from the concentrators) as a function of the normalized distance from the notch root along the bisector, notated  $x$ , to the notch root radius as  $R$  for the semicircular concentrator, and  $r$  for the V-notched specimens. In the numerical analyses we show the corresponding plots on the surface and in the midplane.

#### a) Specimen with two semicircular notches and radius $R = 3$ mm

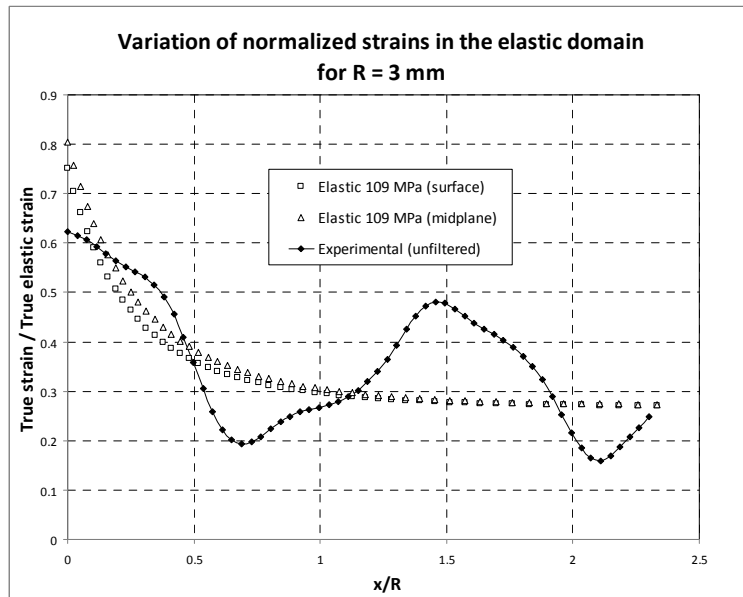
In the linear elastic domain, for a nominal stress of 109 MPa, in Fig. 7a) it is to be noticed that the strains established by DIC show a lot of noise due to the low level of loading. By filtering these experimental values we obtain their decrease, which is not desirable. The experimental and numerical variations of the normalized true strains as a function of the normalized distance from the notch root are represented in Fig. 7b) for the same load level. Finite element strains on the surface and in the midplane are about the same and a little bit greater than the experimental strains at the root of the notch. The true elastic strain is established from the true stress-strain diagram of the specimen without a notch and considering the elastic stress of 260 MPa as the upper limit for the elastic domain. At this limit, in fact being in between the elastic and plastic domains, in Fig. 7c) are shown the same variations as before, but only with the unfiltered experimental normalized strains. The experimental results are very close to the numerical ones, which give now a difference in between the surface and midplane values, the last being greater. The variation of the normalized experimental strains still show some noise, especially further away from the notch tip where true strains are of lower values. At a distance from the notch root up to  $x/R < 0.5$  the influence of the concentrator is important as normalized strains are greater than 1 although the load level is, theoretically, still in the elastic domain. The elastic numerical strains are smaller than the so-called elasto-plastic ones showing that a zone of length half the radius of the notch is already under the strong influence of the notch.

At a load level of 463 MPa, very close to the failure of the notched specimen (Fig. 7d), the experimental normalized strains are much greater than the numerical ones, both at the notch root and over the whole ligament. These strains show now a

smooth variation and extensive yielding in the whole net section in between the two semicircular notches.



a)



b)

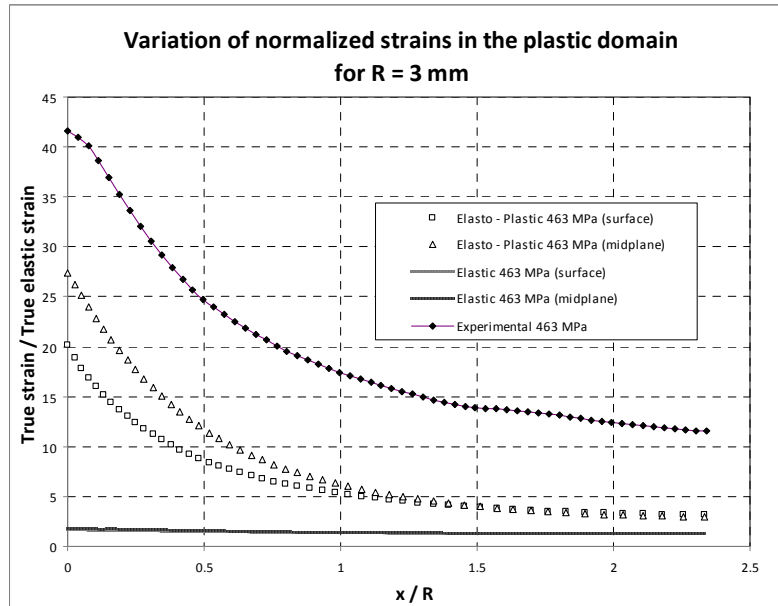
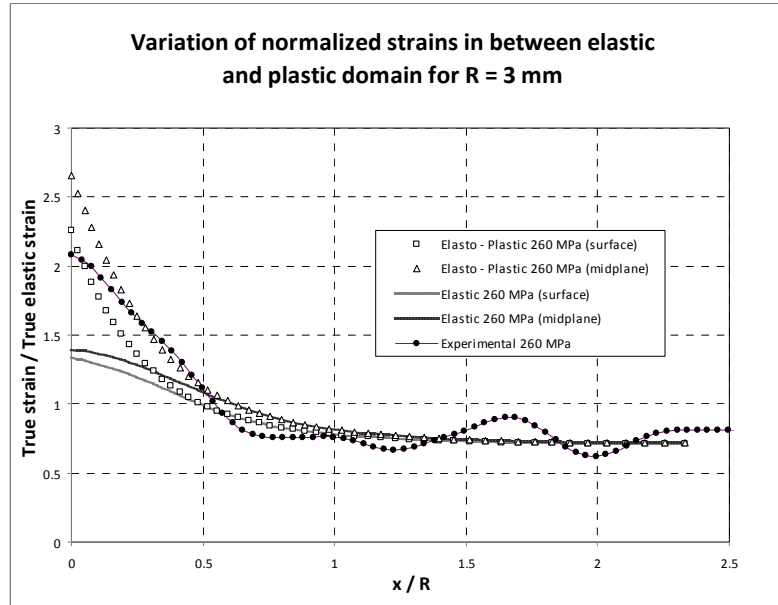
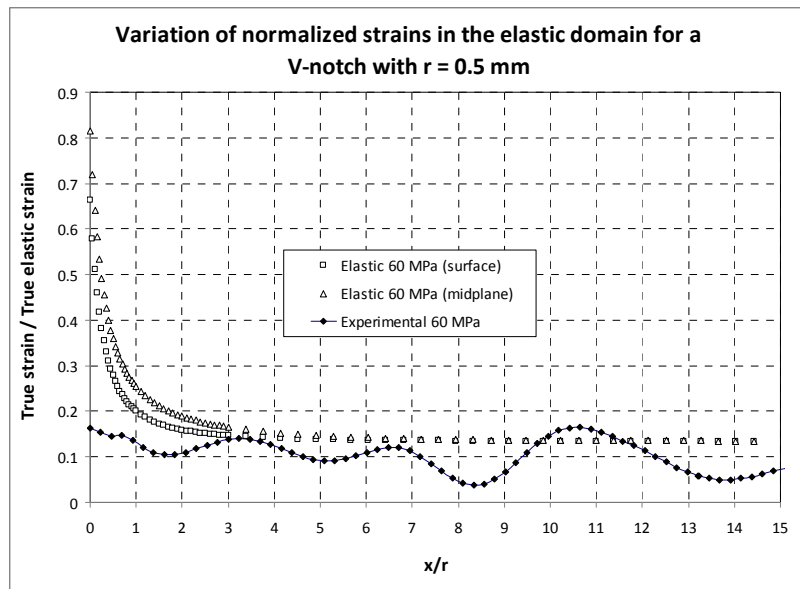


Fig. 7 – Comparison of strains variations along the notch bisector for a semicircular concentrator:  
 a) elastic true strains variation; b) elastic normalized true strains; c) elastic and elasto-plastic normalized true strains; d) plastic normalized true strains.

### b) Specimen with two V-notches and root radius $r = 0.5$ mm

This time, in the linear elastic domain, the variation of normalized strains is represented at a nominal stress of 60 MPa (Fig. 8a). Again, quite a lot of noise is present and the unfiltered strains obtained experimentally by DIC are, in general, smaller than the ones obtained with finite elements. Difference in between the finite element normalized strains in the surface plane and midplane is obtained up to  $x/r = 3$ . Also up to this normalized distance from the root of the V-notch the experimental normalized strains are much smaller than the numerical ones. For  $x/r > 3$ , normalized strains are about the same, but, clearly the noise in the experimental results does affect the smoothness of longitudinal strain variation. In Fig. 8b, experimental normalized strains are much smaller than the numerically obtained ones up to  $x/r = 3$ . Experimental true strain ratio at the tip of the V-notch is 2, compared to a numerical value of 7 in the midplane and a value of about 4.5 on the outer surface, where in fact comparison should be done. However, just on the outer surface of the notch the resolution of DIC in establishing strains is limited as the speckle pattern is blurred. Beyond the ratio  $x/r = 3$  all normalized strains are practically the same. In the elasto-plastic domain (Fig. 8 c), for a stress of 435 MPa, experimental true strain ratio at the tip of the V-notch is 15 compared to a numerical value of about 20 on the outer surface. For  $x/r > 1$  experimental normalized longitudinal strains along the bisector get very close to the finite element normalized strains in the midplane, and for  $x/r > 3$  (1.5 mm) become greater than the numerical values, as in the case of a semicircular notch.



a)

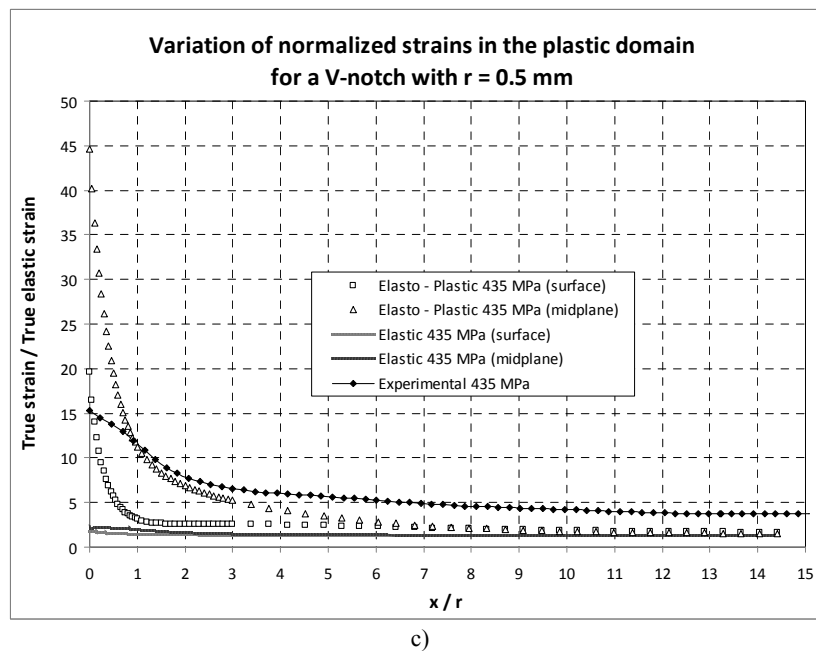
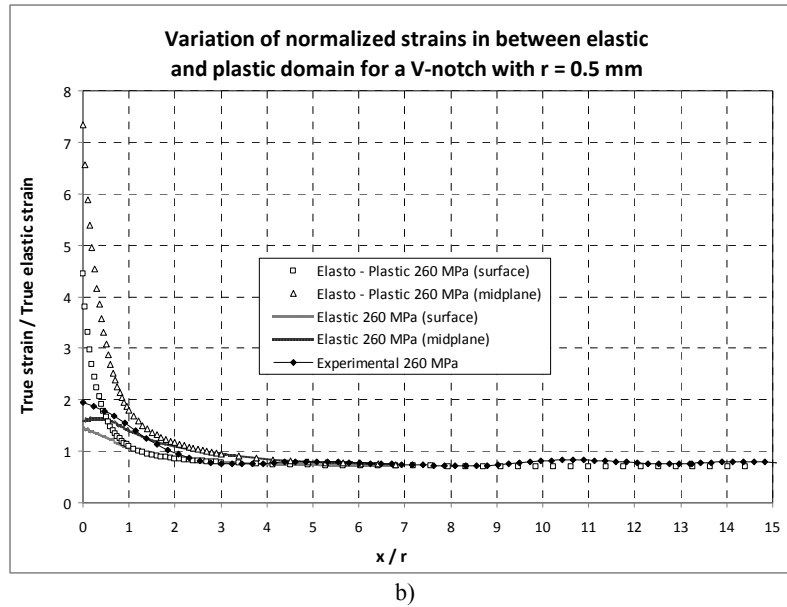
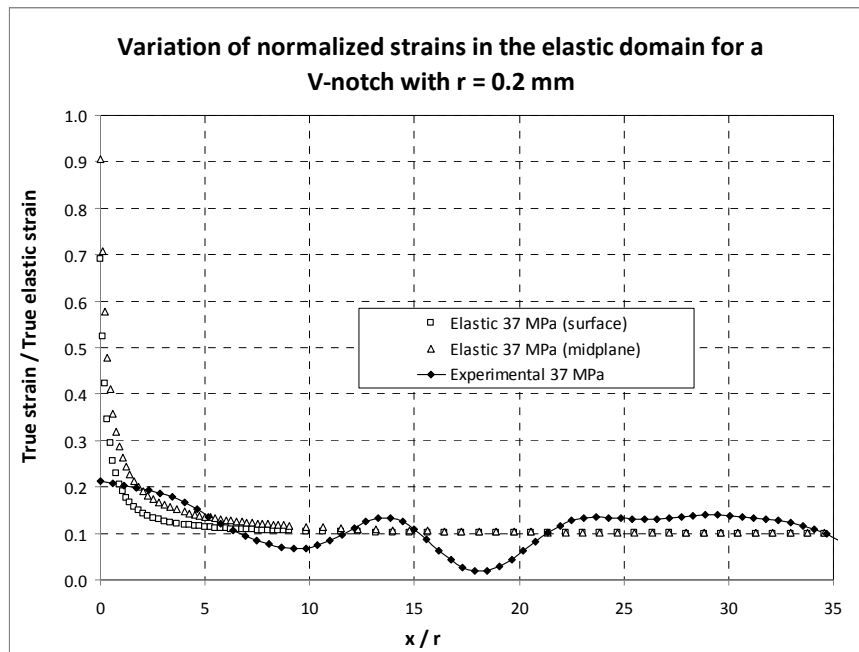


Fig. 8 – Comparison of strains variations along the notch bisector for a V-notch with radius  $r = 0.5$  mm: a) elastic normalized true strains; b) elastic and elasto-plastic normalized true strains; c) plastic normalized true strains.

### c) Specimen with two V-notches and root radius $r = 0.2$ mm

At 37 MPa the normalized strains are shown in Fig. 9a. Very close to the V-notch root the normalized numerical strains are having a value of 0.9 in the midplane, and 0.7 on the surface of the specimen, compared to a ratio of 0.2 obtained experimentally. For a normalized distance from the V-notch root  $x/r > 1.7$  experimental normalized strains in the linear elastic domain are about the same as the numerical ones. The waviness aspect seen in the strains variation is present again due to the noise registered at this low level of loading. At the limit in between the elastic domain and the plastic domain (Fig. 9b), that is at 260 MPa, the normalized strains obtained experimentally have a value of 2 at the base of the notch, as for the V-notch with  $r = 0.5$  mm. Beyond  $x/r = 2.3$  the experimental and finite element normalized strains are almost the same. Finally, in the plastic domain, at a stress of 416 MPa (Fig. 9c), experimental strains are again smaller than the numerical ones at the base of the notch, but for  $x/r > 2.3$  experimental values are identical with the numerical ones in the midplane, and for  $x/r > 10$  (that is 2 mm) exceed a little bit the finite element normalized strains.



a)

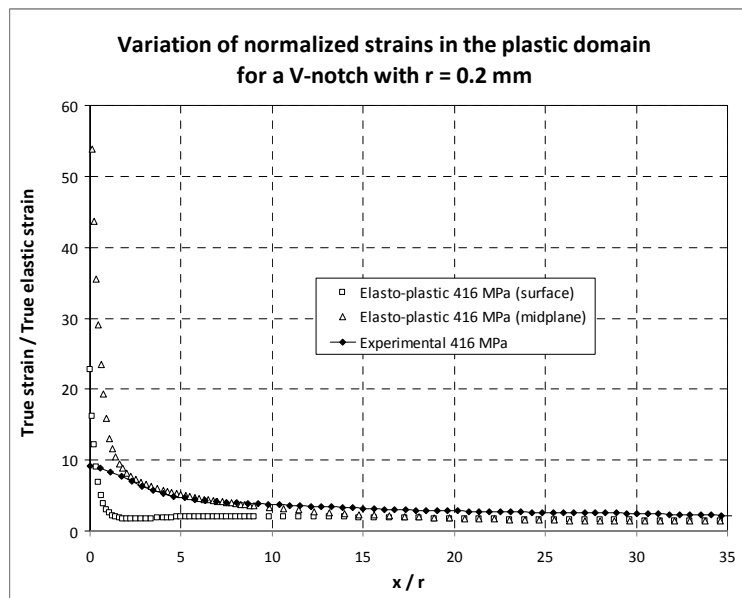
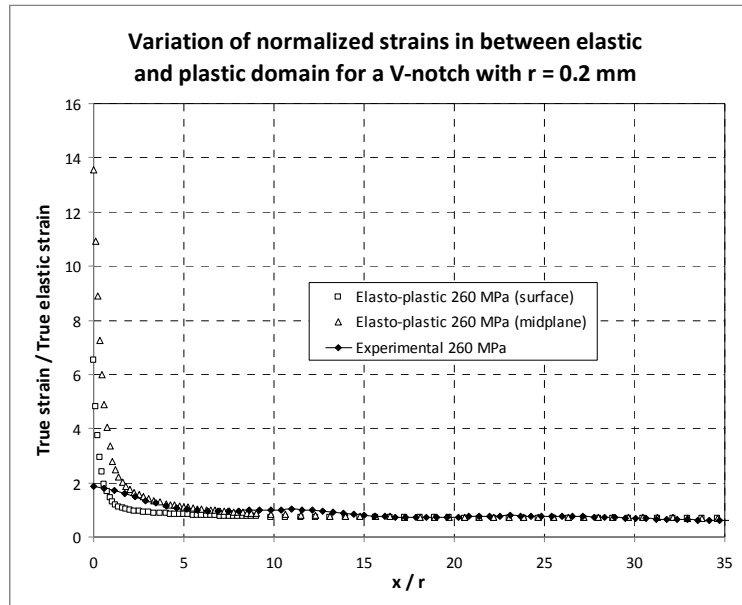


Fig. 9 – Comparison of strains variations along the notch bisector for a V-notch with radius  $r = 0.2$  mm: a) elastic normalized true strains; b) elastic and elasto-plastic normalized true strains; c) plastic normalized true strains.

### 5. EVALUATION OF STRAIN CONCENTRATION FOR V-NOTCHES

Filippi *et al.* [11] solution in the linear elastic domain proved to be efficient by adding a potential function to the previous solution of Lazzarin and Tovo [6], being therefore capable to improve the term that has influence on the stress distribution close to the notch tip. Although approximate, its efficiency has been demonstrated for different V-notches as being sharp or rounded, and different notch angles. For a notch angle  $2\alpha = 90^\circ$  (as for our tested specimens), the circumferential normal stress along the notch bisector (for  $\theta = 0$ ), as a maximum principal stress, can be expressed with the relation

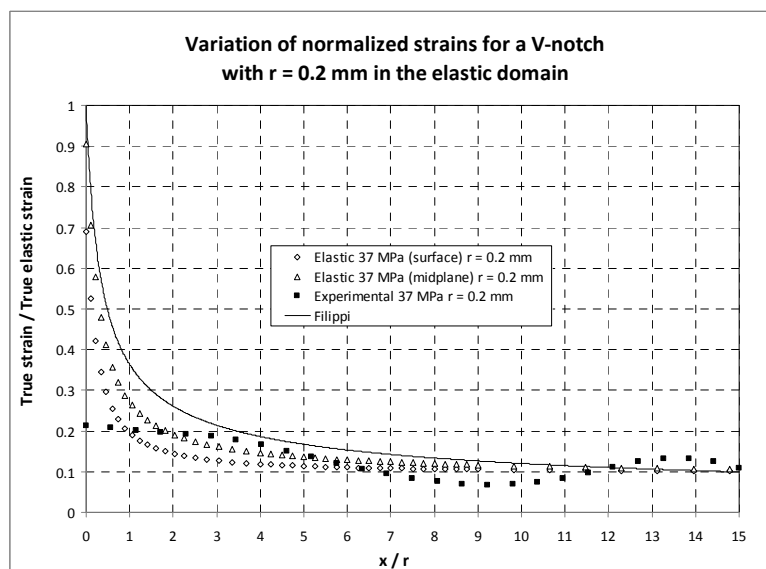
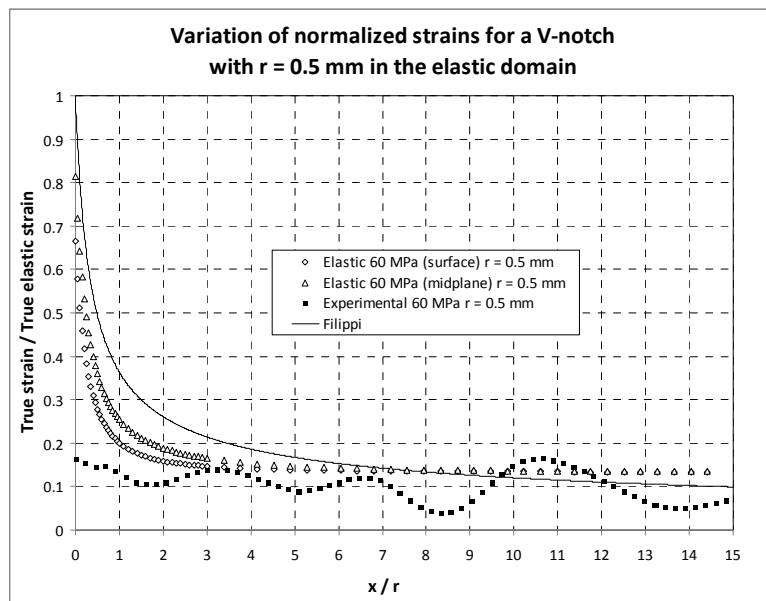
$$(\sigma_\theta)_{\theta=0} = \frac{\sigma_{\max}}{3.874} \rho^{0.4555} \left[ 1.2976(x + 0.3333\rho)^{-0.4555} + 0.3957\rho^{0.8894} (x + 0.3333\rho)^{-1.3449} \right], \quad (1)$$

where  $\sigma_{\max}$  is at the limit the maximum elastic stress,  $\rho$  is the V-notch root radius and  $x$  is the distance from the notch root measured along the bisector.

This equation can be rewritten in terms of the ratio between the true strain at notch root to the maximum true elastic strain obtained for a conventional stress of 260 MPa – being the limit for the elastic domain, as to be able to compare it with the previously obtained values through DIC and finite element calculations. In Fig. 10 a and b, Filippi's equation is plotted and compared with our results in the linear elastic domain for the two V-notches, having radii  $r = 0.5$  mm, and respectively  $r = 0.2$  mm. Filippi's curve is above the finite element results for both outer surface and midplane chosen for the representation of the normalized true strains. Experimental normalized strains obtained with DIC are, as commented before, lower than the finite element values close to the notch root, and about the same as  $x/r > 3$ ; a better comparison of all data is obtained for the V-notch with  $r = 0.2$  mm – in fact experimental data show less noise as being filtered.

For the load in between the elastic domain and the plastic domain, at a stress of 260 MPa, we compare on the surface of the specimens the normalized true strains obtained for both V-notches with DIC and finite elements (FE). In Fig. 10c it is to be seen that very close to the notch base the numerical values prevail. From  $x/r > 0.7$  experimental normalized strains are greater or equal with the numerical ones, especially for the V-notch with  $r = 0.2$  mm. For  $x/r > 5$  and up to  $x/r = 15$  – that is towards the axis of symmetry of the specimens – the numerical values of the normalized strains are practically the same. If  $x/r > 5$  the ratio of the normalized experimental strains is equal to 1 for  $r = 0.2$  mm, and bellow 1 for  $r = 0.5$  mm.

In Fig. 10d, it is shown the comparison (on the surface of the specimens) of the experimental normalized true strains in the plastic domain at a stress of 435 MPa for  $r=0.5$  mm and 416 MPa for  $r=0.2$  mm, and of the corresponding FE



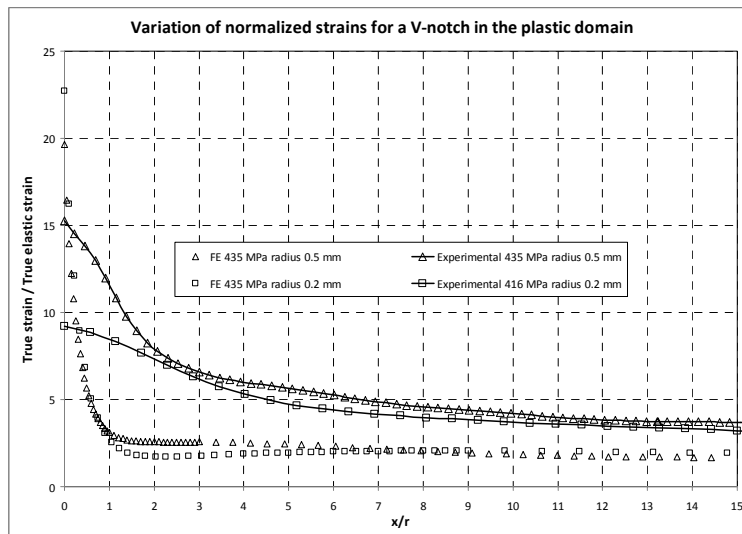
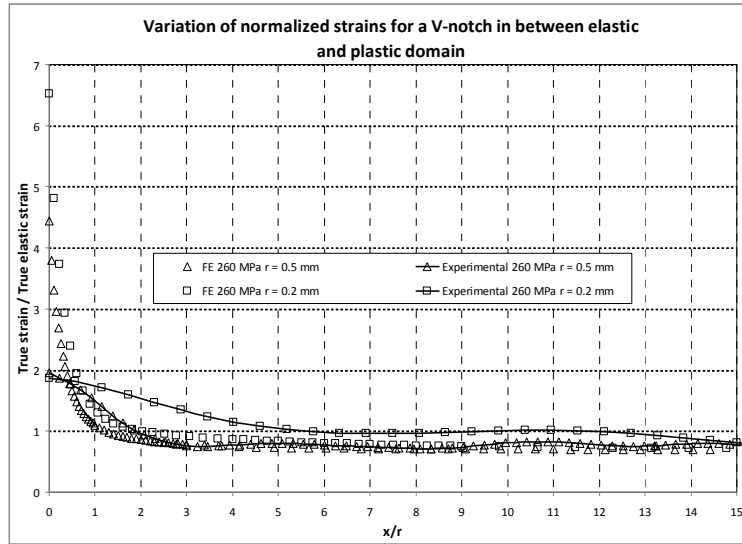


Fig. 10 – Variation of normalized true strains for V-notches: a) elastic domain  $r = 0.5$  mm; b) elastic domain  $r = 0.2$  mm; c) elasto-plastic domain for  $r = 0.5$  mm and  $r = 0.2$  mm; d) plastic domain for  $r = 0.5$  mm and  $r = 0.2$  mm.

normalized strains for a stress of 435 MPa. Already from  $x/r > 0.6$  experimental normalized strains are greater than the numerical ones. Experimental normalized strains for  $r = 0.2$  mm are smaller than for  $r = 0.5$  mm, but the stress is also smaller. From  $x/r > 2$  the experimental normalized strains are almost the same,

but significantly greater than the numerically obtained ones. Normalized FE true strains are mostly equal for both V-notches with a small difference where  $x/r$  is in between 1 and 5, where the notch with  $r = 0.5$  mm gives greater values. It is important to underline that the yielding in the ligament is much stronger in reality – as measured with DIC – than predicted by FE simulations. The ratio of the true experimental normalized strains is about 4, as compared to the same ratio obtained by FE which is about 2. Closer to the V-notches root, from  $x/r > 1$ , the difference is much bigger up to  $x/r = 4$ , with the ratio of the conventional experimental normalized strains decreasing from 11 to 5, compared with the ratio of the FE normalized strains of about 2.5–3.0.

## 6. CALCULATION OF THE ELASTO-PLASTIC STRAIN CONCENTRATION FACTORS THROUGH DIGITAL IMAGE CORRELATION

We are interested to analyze the strain concentration factor in the elasto-plastic domain. The aluminum 2024-T3 follows a hardening Ramberg-Osgood law, having an offset yield limit of 340 MPa. The acquired experimental and numerical data are obtained till the failure of the specimens with symmetrical three distinctive concentrators, which are considered in what follows as left and right. We have seen in Fig. 10 c and d that, due to plastic relaxation, the maximum strains at the root of the V-notches is smaller than the numerically predicted ones, but greater as we move away along the ligament.

We may define two types of strain concentrators: a *nominal* one, for which we divide the conventional strains at the notch root at different load levels to the nominal conventional strain which results at the same load level in the gross section without concentrator, and another called *effective* for which we divide the notch strains to the average strain measured in the middle of the specimen along 6 mm, as being the height of all three analyzed concentrators. In this way we reiterate a similar idea presented by Boresi et al. [36] who introduce the concept of the *effective stress concentration factor* for an ideal elastic material. This time the material hardens, and the effects of yielding have to influence the effect of strain concentration. When calculating the *nominal strain concentration factor* we use as reference a pseudo-elastic nominal conventional strain by dividing the stress at each load level to the longitudinal modulus of elasticity. In this way we can get a global variation of the strain concentration both in the elastic domain and plastic domain as a function of the ratio between the actual stress and the offset yield limit ( $\sigma/\sigma_y$  in which  $\sigma_y$  is in fact  $\sigma_{0.2}$ ) established experimentally. For the *effective strain concentration factor* the conventional local strains at the base of the notch for different load levels are divided to the strain measured along the axis of symmetry of the specimen, far away from the concentrators, but in the same time being on the yielded ligament.

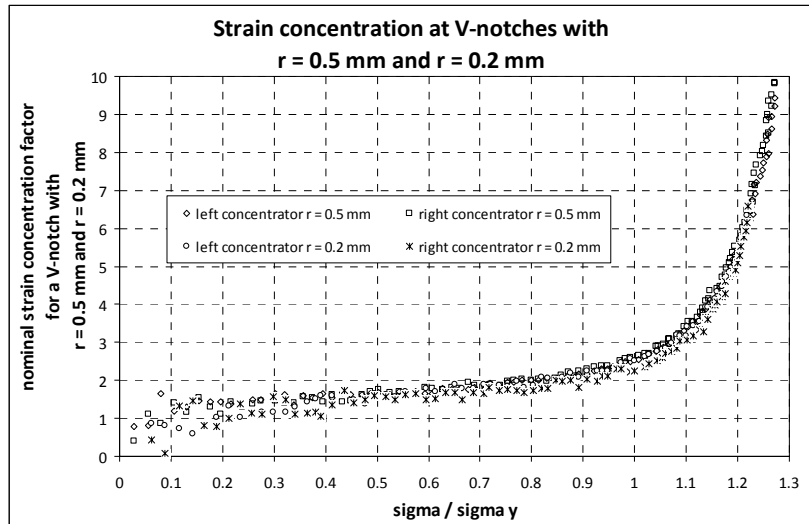


Fig. 11 – Variation of nominal strain concentration factor for V-notches.

Therefore, for the V-notch concentrators we divide the left and right measured with DIC conventional strains – as close as possible from the base of the notch – to the nominal elastic conventional strain averaged over the gross section and calculated by considering the stress at each load level divided to  $E=67.85$  MPa, Young's modulus obtained by us experimentally. The *nominal strain concentration factor* variation is shown in Fig. 11 for both V-notches, left and right. For a load level  $\sigma/\sigma_y < 0.4$  (notated in the figure sigma/sigma y) the dispersion of experimental data is significant, showing that at low load levels the resolution of the measurements at the boundary of the notch is influenced strongly by the induced noise. When loading is increased data start to get unified on the same trend of variation and, as yielding is produced, the variation becomes steeper till the failure of the specimens for this material being attained for  $\sigma/\sigma_y$  at most equal to 1.27 for the V-notch with  $r=0.5$  mm as having a nominal strain concentration factor as 9.81 at the right concentrator and 9.44 at the left concentrator. For the V-notch with  $r=0.2$  mm the nominal strain concentration factor is 6.58 at the right concentrator and 6.49 at the left concentrator

We can also represent on the same plot the nominal strain concentration factor for all three geometries as in Fig. 12. It is interesting to notice that even if maximum values are not the same (for semicircular notch being 7.43 at left strain raiser and 6.78 at the right one) the trend of variation is identical and data superpose nicely beyond  $\sigma/\sigma_y = 0.4$ , when the resolution of the experimental measurements with digital image correlation increases. A parabolic fit of all data shows that a third order equation is appropriate for  $\sigma/\sigma_y > 1$ , and a six order equation can be used for  $\sigma/\sigma_y > 0.4$ .

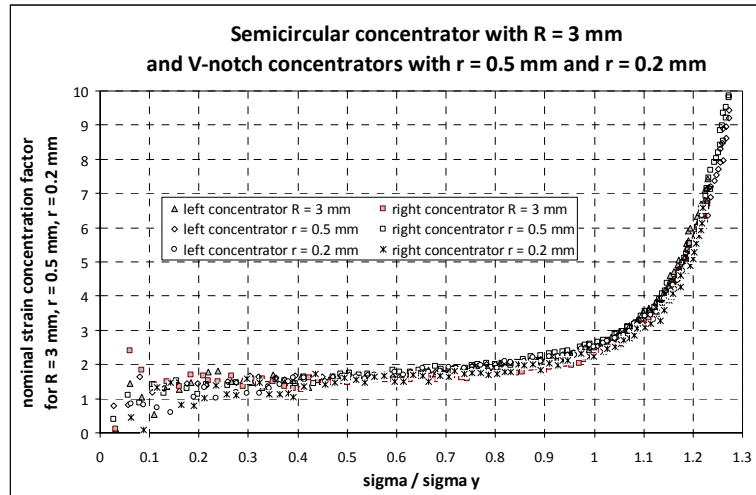


Fig. 12 – Variation of nominal strain concentration factor for all three concentrators.

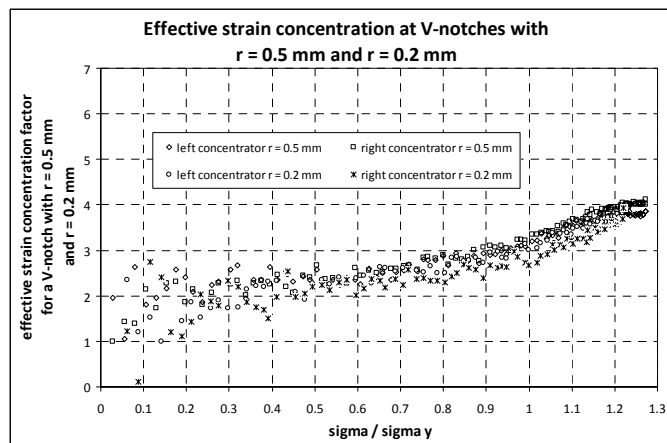


Fig. 13 – Variation of effective strain concentration factor for V-notches.

Another possible interpretation of the results is to calculate the so called *effective strain concentration factor* which is obtained by dividing at each load level the left and right measured strains at the base of the notch to the strain measured experimentally with the virtual strain gage of 6 mm in the middle of the specimen along its longitudinal axis. In Fig. 13 we represent such a variation only for the V-notched specimens. The same significant scatter of data (even greater as before) is obtained up to  $\sigma/\sigma_y < 0.5$ . Beyond the ratio  $\sigma/\sigma_y = 1$  the variation tends to be linear and showing that when reaching the ratio  $\sigma/\sigma_y = 1.2$  the force remains almost constant and, in fact, the effective strain concentration factor doesn't increase any more keeping for both notches a value of about 4. Such an

interpretation is more realistic, taking into account the yielding of the material in the net section where strain raisers are.

## 7. DISCUSSION

In order to summarize we compare the influence of the three notches on the strain distributions in the net sections – along the ligament – in Table 1. In representing the variation of the strain concentration factors (as nominal and effective) we consider them as a function of the ratio between the nominal remote traction stress which is applied and the offset yielding stress established from a tensile test of the specimen without concentrators.

It is interesting to observe that strain at the root of the notches is decreasing from the semicircular ones to the V-notch with  $r = 0.5$  mm and to the V-notch with  $r = 0.2$  mm. That is, as we decrease the notch root, the maximum conventional opening strain measured at the root of the notch (on the notch bisector) is decreasing at failure; the notch becomes sharper, closer to a crack like condition and plastic relaxation in front of such a crack-like notch is more severe.

Table 1

Notch shape	Strain at the root of the notch before failure [%]*		Nominal strain concentration factor at $\sigma/\sigma_y = 1$		Nominal strain concentration factor at failure		Effective strain concentration factor at failure	
	left	right	left	right	left	right	left	right
Maximum $\sigma/\sigma_y = 1.36$								
Semicircular $R = 3$ mm	16.15	13.77	2.62	2.36	23.68	20.19	3.46	2.95
Maximum $\sigma/\sigma_y = 1.27$								
V- $r = 0.5$ mm	6.02	6.26	2.53	2.63	9.44	9.81	3.85	4.00
Maximum $\sigma/\sigma_y = 1.22$								
V- $r = 0.2$ mm	3.97	4.03	2.52	2.24	6.49	6.59	3.87	3.93

\* Strain along the notch bisector

It is interesting to notice that at the limit of the linear elastic domain the nominal strain concentration factor is not too much different for all three notches. The main question is opened: is such a calculation relevant?

The specimen with semicircular strain raisers fails at  $\sigma/\sigma_y = 1.36$  at a nominal strain concentration factor above 20, being calculated with respect to an elastic strain established in the nominal section. For the V-notches this factor decreases to about 9.6 in average for  $r = 0.5$  mm, and to 6.5 for  $r = 0.2$  mm at maximum  $\sigma/\sigma_y$  which are about the same, but decreasing a little bit (Table 1). Conventional maximum strain before failure at the base of the semicircular notch is more localized along the notch bisector and is in average 15%, being less distributed on

the ligament towards the axis of symmetry of the specimen. For  $r = 0.5$  mm the nominal strain concentration factor at failure decreases to an average value of 9.6. The maximum strain just before failure is on an inclined line and of value 6.355 %, with smaller, but about the same values (6.02 left and 6.26 right), along the ligament. The specimen fails faster, at  $\sigma/\sigma_y = 1.27$ , as the notch induces a more severe concentration. Strain concentration localizes differently for the sharper V notch with  $r = 0.2$  mm, and the maximum strain reaches a value of 6.319 % on a line inclined with about  $45^\circ$  – value a little bit greater than before – but along the notch bisector the strain at failure is decreased to about 4 %. The specimen breaks at  $\sigma/\sigma_y = 1.22$  with strain concentration factors of 6.49 at left and 6.59 at right, smaller with about 50 % as compared to the previous values for  $r = 0.5$  mm (Table 1). This doesn't mean that the V-notch with a smaller root radius is less aggressive; it only means that strain redistribution is different. So, there is a tough competition in between these two V-notches just before the failure of the specimens.

Coming back to the calculation of an *effective strain concentration factor* and to Fig. 13, the phenomena of strain concentration is linearized in the zone of hardening and before the failure of the specimens (as we reach the plateau region of the conventional stress-strain curve) such an elasto-plastic strain concentration factor remains mainly constant. Table 1 gives these values for all three notches. For the V-notches the average value of 4 is to be calculated. So, although strain redistribution along the notch bisector is different for the two radii, when the condition of generalized yielding before failure is reached the effects of strain concentration are about the same. As it should be, the effective strain concentration factor for the V-notches is greater than for the semicircular notches. We have to remember that, on the contrary, the nominal strain concentration factor calculated in the elasto-plastic domain but on linear elastic bases is greater for the semicircular notch. This is of course very much disputable.

## 8. CONCLUSIONS

Digital image correlation (DIC) and three-dimensional finite element (FE) investigations are used to analyze the strain fields and the strain concentration factors for three notches: one semicircular with a radius  $R = 3$  mm, and two V-notches with radii  $r = 0.5$  mm and  $r = 0.2$  mm. The tested material is 2024-T3 aluminum which follows a hardening rule of Ramberg-Osgood type.

For each tested notched specimen analyses were done both in the elastic and elasto-plastic domains. Results obtained experimentally with DIC and with FE are compared in the same plots. The ratio of the normalized true opening strains to the true elastic strains as a function of the normalized distance from the notch root along the bisector, notated  $x$ , to the notch root radius is represented. In the linear elastic domain a comparison to Filippi's solution for V-notches is also done, the theoretical corresponding curve being an upper bound.

The main focus of the analyses of these notches is to establish the strain variation in the elasto-plastic domain by comparing the normalized opening strain fields obtained with DIC and 3D finite elements (on the surface plane), along the notch bisector. Generally, in the elasto-plastic domain the experimental normalized strains are much greater than the numerical ones, both at the notch root and over the whole ligament. For the V-notches starting from  $x/r > 0.6$  experimental normalized strains are greater than the numerical ones. From  $x/r > 2$  the experimental normalized strains are almost the same, but significantly greater than the numerically obtained ones. Normalized FE true strains are mostly equal for both V-notches with a small difference where  $x/r$  is in between 1 and 5 where the notch with  $r = 0.5$  mm gives greater values. It is important to underline that the yielding in the ligament is much stronger in reality – as measured with DIC – than predicted by FE simulations.

The digital image correlation method proves to be very efficient when establishing strains at the root of notches both in elastic and elasto-plastic domains. Valuable information is obtained on the strain distribution at the root of the notches, and makes possible the calculation of a *nominal strain concentration factor*. When calculating this value, the left and right measured strains (as close as possible to the root of the notch) are divided to the nominal conventional strain averaged over the entire gross section and calculated by considering the stress at each load level divided to the Young's modulus obtained by us experimentally. In this way we can get a global variation of the strain concentration both in the elastic domain and plastic domain as a function of the ratio between the actual stress and the offset yield limit established experimentally. Another possible interpretation is to calculate an *effective strain concentration factor* which is obtained by dividing at each load level the left and right measured strains at the root of the notch to the strain measured experimentally with a virtual strain gage of 6 mm considered in the middle of the specimen along its longitudinal axis of symmetry; this gives a localized, more correct, strain value in the net section indicating also the yielding produced along the ligament. All comments presented in our discussion emphasize that the calculation of an *effective strain concentration factor* is much closer to real phenomena and recommended to be used.

For the V-notches it results also that strain distribution in the elasto-plastic domain is different very close to the notch root but about the same further away, along the ligament.

*Received on December 16, 2010*

#### REFERENCES

1. WESTERGAARD, H.M., *Bearing pressures and cracks*, Journal of Applied Mechanics, **6**, A49–53, 1939.
2. IRWIN, G.R., *Analysis of stresses and strain near the end of a crack transversing a plate*, Journal of Applied Mechanics, **24**, pp. 361–364, 1957.

3. WILLIAMS, M.L., *Stress singularities resulting from various boundary conditions in angular corners of plates in tension*, Journal of Applied Mechanics, **19**, pp. 526–528, 1952.
4. CREAGER, M., PARIS, P.C., *Elastic field equations for blunt cracks with reference to stress corrosion cracking*, International Journal of Fracture Mechanics, **3**, pp. 247–252, 1967.
5. GLINKA, G., *Calculation of inelastic notch-tip strain-stress histories under cyclic loading*, Engineering Fracture Mechanics, **22**, pp. 839–854, 1985.
6. LAZZARIN, P., TOVO, R., *A unified approach to the evaluation of linear elastic fields in the neighborhood of cracks and notches*, International Journal of Fracture, **78**, pp. 3–19, 1996.
7. LAZZARIN, P., TOVO, R., FILIPPI, S., *Stress distribution in finite size plates with edge notches*, International Journal of Fracture, **91**, pp. 69–282, 1998.
8. GLINKA, G., NEWPORT, A., *Universal features of elastic notch-tip stress fields*, International Journal of Fatigue, **9**, pp. 143–150, 1987.
9. XU, R.X., THOMPSON, J.C. AND TOPPER, T.H., *Practical stress expressions for stress concentration regions*, Fatigue and Fracture of Engineering Materials and Structures, **18**, pp. 885–895, 1995.
10. KUJAWSKI, D., SHIN, C.S., *On the elastic longitudinal stress estimation in the neighbourhood of notches*, Engineering Fracture Mechanics, **56**, pp. 137–138, 1997.
11. FILIPPI, S., LAZZARIN, P., TOVO, R., *Developments of some explicit formulas useful to describe elastic stress fields ahead of notches in plates*, International Journal of Solids and Structures, **39**, pp. 4543–4565, 2002.
12. BERTO, F., LAZZARIN, P., RADAJ D., *Fictitious notch rounding concept applied to sharp V-notches: Evaluation of the microstructural support factor for different failure hypotheses. Part I: Basic stress equations*, Engineering Fracture Mechanics, **75**, pp. 3060–3072, 2008.
13. NEUBER, H., *Theory of Notch Stresses*, Springer-Verlag, Berlin, 1958.
14. NEUBER H., *Theory of stress concentration for shear-strained prismatical bodies with arbitrary nonlinear stress strain law*, Journal of Applied Mechanics, **26**, pp. 544–550, 1961.
15. LI, Z., GUO, W., KUANG, Z., *Three-dimensional elastic stress fields near notches in finite thick plates*, International Journal of Solids and Structures, **37**, pp. 7617–7631, 2000.
16. LI, Z., GUO, W., *Three-dimensional elastic stress fields ahead of blunt V-notches in finite thickness plates*, International Journal of Fracture, **107**, pp. 53–71, 2001.
17. KOTOUSOV, A., WANG, C.H., *Three dimensional stress constraint in an elastic plate with a notch*, International Journal of Solids and Structures, **39**, pp. 4311–4326, 2002.
18. HUTCHINSON, J.W., *Singular behavior at the end of a tensile crack in a hardening material*, Journal of the Mechanics and Physics of Solids, **16**, pp. 13–31, 1968.
19. RICE, J.R., ROSENGREN G.F., *Plane strain deformation near a crack tip in a power-law hardening material*, Journal of the Mechanics and Physics of Solids, **16**, pp. 1–12, 1968.
20. LAZZARIN, P., ZAMBARDI, R., LIVIERI, P., *Plastic notch stress intensity factors for large V-shaped notches under mixed load conditions*, International Journal of Fracture, **107**, pp. 361–377, 2001.
21. GROSS, R., MENDELSON, A., *Plane elastostatic analysis of V-notched plates*, International Journal of Fracture Mechanics, **8**, pp. 267–27, 1972.
22. MOLSKI, K., GLINKA, G., *A method of elastic-plastic stress and strain calculation at a notch root*, Material Science Engineering, **50**, pp. 93-100, 1981.
23. LAZZARIN, P., ZAMBARDI, R., *The equivalent strain energy density approach re-formulated and applied to sharp V-shaped notches under localized and generalized plasticity*, Fatigue and Fracture of Engineering Materials and Structures, **25**, pp. 917–928, 2002.
24. SETHURAMAN, R., VISWANADHA, S., *Evaluation of notch root elasto-plastic stress-strain state for general loadings using an elastic solution*, International Journal of Pressure Vessels and Piping, **81**, pp. 313–325, 2004.
25. SINGH, M.N.K., GLINKA, G., DUBEY, R.N., *Elastic-plastic stress-strain calculation in notched bodies subjected to non-proportional loading*, International Journal of Fracture, **76**, pp. 39–60, 1996.

26. GÓMEZ, F.J., ELICES, M., BERTO, F., LAZZARIN, P., *A generalized notch stress intensity factor for U-notched components loaded under mixed mode*, Engineering Fracture Mechanics, **75**, pp. 4819–4833, 2008.
27. GÓMEZ, F.J., ELICES, M., BERTO, F., LAZZARIN, P., *Fracture of U-notched specimens under mixed mode experimental results and numerical predictions*, Engineering Fracture Mechanics, **76**, pp. 236–249, 2009.
28. GÓMEZ, F.J., ELICES, M., BERTO, F., LAZZARIN, P., *Fracture of V-notched specimens under mixed mode (I + II) loading in brittle materials*, International Journal of Fracture, **159**, pp. 121–135, 2009.
29. KIM, J.K., CHO, S.B., *A unified brittle fracture criterion for structures with sharp V-notches under mixed mode loading*, Journal of Mechanical Science and Technology, **22**, pp. 1269–1278, 2008.
30. SUSMEL, L., TAYLOR, D., *Two methods for prediction the multiaxial fatigue limits of sharp notches*, Fatigue and Fracture of Engineering Materials and Structures, **26**, pp. 821–833, 2003.
31. SUTTON, M.A., ORTEU, J.-J., SCHREIER, H., *Image Correlation for Shape, Motion and Deformation Measurements; Basic Concepts, Theory and Applications*, Springer, Berlin, 2009.
32. MEKHY, W., NICHOLSON, P.S., *The fracture toughness of Ni/Al<sub>2</sub>O<sub>3</sub> laminates by digital image correlation I: Experimental crack opening displacement and R-curves*, Engineering Fracture Mechanics, **73**, pp. 571–582, 2006.
33. CARROLL J., EFSTATHIOUS C., LAMBROS J., SEHITOGLU H., HAUBER, B., SPOTTSWOOD, S., CHONA, R., *Investigation of fatigue crack closure using multiscale image correlation experiments*, Engineering Fracture Mechanics, **76**, pp. 2384–2398, 2009.
34. SUTTON M.A., YAN J.H., TIWARI V., SCHREIER H.W., ORTEU J.J., *The effect of out-of-plane motion on 2D and 3D digital image correlation measurements*, Optics and Lasers in Engineering, **46**, pp. 746–757, 2008.
35. YA'AAKOBVITZ A., KRYLOV S.M., HANEIN Y., *Nanoscale displacement measurement of electrostatically actuated micro-devices using optical microscopy and digital image correlation*, Sensors and Actuators A: Physical, **162**, 1, pp. 1–7, 2010.
36. BORESI, A.P., SCHMIDT, R.J., SIDEBOTTOM, O.M., *Advanced Mechanics of Materials*, 5<sup>th</sup> ed., Wiley, New York, 1993.